Theoret. Chim. Acta (Berl.) 34, 199—212 (1974)

Determination of the H_2–H_2 Potential from Absolute Integral Cross Section Measurements*

Rolf Gengenbach**, Christian Hahn***, Wilhelm Schrader****,
and Jan Peter Toennies

Physikalisches Institut der Universität Bonn
and Max-Planck-Institut für Strömungsforschung, Göttingen

Received February 18, 1974

Absolute integral cross sections have been measured for n-H_2–n-H_2 at primary particle velocities between 1270 and 9650 m/sec with a 77 °K target. The number density of target particles was determined with an accuracy of 1 % by the method of dynamic expansion. The velocity dependence of the integral cross section was also measured for the isotopic systems n-D_2–n-H_2 and n-D_2–n-D_2 at primary beam velocities between 280 and 1170 m/sec with a 15 °K target. All available integral cross section data are compared with literature potentials. A new potential is proposed, which exhibits one bound state for H_2–H_2.

Key words: Molecular beam – Absolute integral cross sections – Intermolecular interaction of H_2

Introduction

The H_2–H_2 system is the simplest two molecule system and hence it is of interest from a theoretical as well as from an experimental point of view.

The first attempt to calculate the H_2–H_2 interaction potential was made by de Boer [1a] in a valence bond calculation for the repulsive forces neglecting all non-orthogonality integrals and all triple exchange and quadrupole exchange terms. From a combination of the repulsive and the attractive quadrupole-quadrupole and dispersion forces the potential well was obtained. More refined calculations of Evett and Margenau [1b] and Mason and Hirschfelder [1c] yielded similar results. Recently Kochanski used a similar method for the evaluation of the H_2–H_2 potential well [2]. The most refined valence bond calculations are from Mascagno and Musso [3]. Recently Patch [4] has published valence bond results for the repulsive potential. Vanderslice and Mason [5] obtained a semiempirical H_2–H_2 potential by inserting the values of the exchange integrals derived from the $^1\Sigma$ and $^3\Sigma$ potentials of the H_2 molecule into the Heitler-London formula. A related semiempirical calculation has also been carried out by Abrams *et al.* [6]. No potential well was found in these calculations as in the SCF-calculations of Tapia [7].

CI-calculations were first performed by Wilson and Goddard [8] and Rubinstein and Shavitt [9]. In *ab initio* calculations for the linear H_4 Bender and Schaefer

---

* Dedicated to Professor H. Hartmann on his 60th birthday.

** Present address: Deutsche Forschungsgemeinschaft, 5300 Bonn-Bad Godesberg.

*** Present address: Fakultät für Physik der Universität Bielefeld, 4800 Bielefeld.

**** Present address: 2803 Kirchweyhe, Berliner Str. 16.

[10] found a van der Waals minimum for the first time. Meyer [11] has calculated the H_2–H_2 potential for four geometries by the correlated electron pair approximation (CEPA) and found a potential well which is comparable with the experimental results presented in this paper. Recently the calculations of Rubinstein and Shavitt were extended to a higher degree of accuracy (double zeta) and to more geometrical configurations by Silver and Stevens [12].

Whereas in the intermediate potential range most of the *ab initio* calculations have so far yielded comparatively poor results, the leading dipole-dipole interaction term of the dispersion forces is known from semiempirical calculations within 3% [13] and the uncertainty of *ab initio* values has the same order of magnitude [14].

The first experimental information about the H_2–H_2 potential was obtained from virial and transport coefficients. These data often were fitted with two or three parameter potentials. As Hanley *et al.* have pointed out two different potentials of this type are required to fit the high and the low temperature transport data [15]. This indicates that more flexible potentials are necessary.

The high energy repulsive potential was studied by Leonas *et al.* [16] with Amdur's method of incomplete cross sections. Detailed information about the intermediate potential range is provided by the measurements of the elastic differential cross section of para H_2-para H_2 by Farrar and Lee [17] and of n-H_2–n-H_2 of Dondi *et al.* [18a]. The potentials derived from these measurements are somewhat different. Butz *et al.* have measured the integral cross section for the isotopic systems D_2–D_2, HD–D_2 and HD–HD with an undetermined target density [18b]. Since the integral cross sections of these systems show no interference patterns, only rough estimates of the potential parameters could be deduced from these measurements.

In the present study we have calibrated the measurements of Butz *et al.* by measuring the absolute value of the n-H_2–n-H_2 cross section at several beam velocities. In addition we have measured the velocity dependence of n-D_2–n-H_2 and n-D_2–n-D_2 cross sections at small energies with a 15 °K target. The results of 5 different integral cross section measurements were then used to obtain a best fit Morse-Spline-Van der Waals (MSV) potential.

Experimental Setup and Results

The absolute cross sections were measured in a conventional molecular beam apparatus [19] similar to that used previously [20a, 21] and to be described in detail in [22a] (Fig. 1). The unscattered primary beam particles were velocity selected by a standard mechanical velocity selector with a resolution $\frac{\Delta v}{v} = 0.25$ (FWHM). The target chamber was a double walled container. The region between the walls was filled with liquid N_2 so that the target temperature was constant and equal to the boiling point of liquid N_2 (77.3 °K). The number density n_2 of particles was produced and measured by the method of dynamical expansion [22b]. The beam entrance and exit holes were thin orifices with known conductance for molecular flow. The integral of the number density of target particles over the beam path $\int n_2(x)dx$ was known within 1%. The absolute

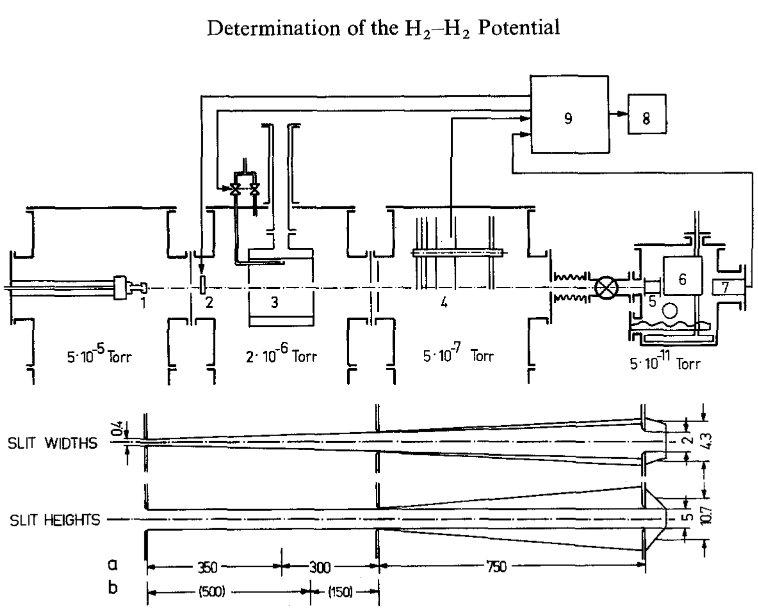

Fig. 1. Schematic view of the apparatus and the beam defining geometry (all distances in mm) for the measurement of the absolute values a) and relative values b). 1: electron bombardment oven, 2: beam flag, 3: target with calibrated holes, 4: velocity selector, 5: ion source, 6: Wien-filter, 7: multiplier, 8: on-line computer PDP8/L, and 9: program timing and data acquisition

accuracy of the number density determination was confirmed in similar studies of He–He scattering [22a]. The measured absolute cross sections for this system have recently been found to be in excellent agreement with those calculated from a potential derived independently from an "inversion" of symmetry undulations [23].

The low energy measurements of the velocity dependence of the integral cross sections were performed in the apparatus of Bennewitz *et al.* [24], which corresponds to our arrangement and is designed for lower energies with higher energy resolution. The mechanical velocity selector has a resolution of 0.125 (FWHM). The target was cooled by a He cryostat to 15 °K. The holes of the target were not calibrated; therefore the target number density was not known absolutely.

The absolute results are listed in Table 1 as mean values of N single measurements. The error given is the statistical error of the mean value. The new relative results are shown in Fig. 2 together with the measurements of Butz *et al.*

Table 1. Measured effective cross sections $\bar{\sigma}$ for H_2–H_2 at primary velocity v, corresponding to center-of-mass energies E_{cm} $(= 1/2\mu v^2)$ with the statistical standard deviation $\Delta\bar{\sigma}/\bar{\sigma}$ of the mean based on N single measurements. σ^+ is the value of $\bar{\sigma}$ corrected for the experimental conditions of 77 °K target and 290–2800 °K oven temperature, 25% velocity resolution (FWHM) and the angular resolving power of the apparatus. σ^+ can be compared directly with quantum mechanical calculations of $\sigma(E_{cm})$ without further averaging

v [m/s]	E_{cm} [meV]	$\bar{\sigma}$ [Å^2]	N	σ^+ [Å^2]	$\Delta\bar{\sigma}/\bar{\sigma}$%
1270	8.4	107.88	45	103.33	0.36
2520	32.9	65.25	69	64.31	0.19
9650	483.0	42.60	67	45.02	0.20

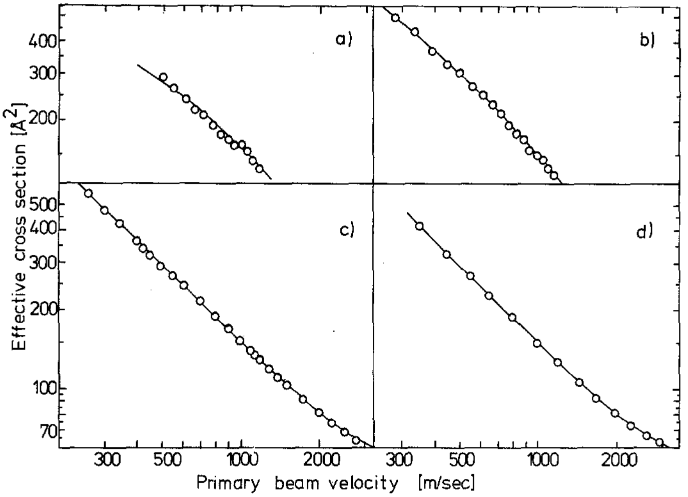

Fig. 2. The measured velocity dependence of total integral cross sections of the H_2–H_2 isotopic systems are compared with our MSV potential. Parts a and b show values measured with a 15.1 °K target (this work) for D_2–D_2 and D_2–H_2, respectively. The values in parts c and d are measured by Butz *et al.* with a 90 °K target for D_2–D_2 and HD–D_2, respectively. The curves are effective cross sections computed with our MSV potential. The close agreement between measured and computed values demonstrates that no significant isotopic effect is present in these measurements

Determination of the Spherical Symmetric Potential V(R)

In interpreting the results in terms of a spherical symmetric potential the question arises as to the extent in which the potential anisotropy effects the measured cross sections. To answer this question an exact close coupling solution of the scattering problem is required. Such calculations are not available. Davison [25a, b] has, however, formulated the problem in the distorted wave approximation. The results indicate that for collisions involving only identical $j=0$ molecules at energies below the inelastic threshold only the spherically symmetric part of the potential contributes to the integral cross section. At higher energies inelastic channels make a contribution. The $0 \rightarrow 2$ inelastic cross section has been found to rise linearly with energy and is 0.5 Å^2 at $E_{\mathrm{cm}} = 0.3$ eV [25c]. The other inelastic cross sections are expected to be smaller. Another small contribution to the total cross section from the anisotropic potential will result from the matrix elements associated with the transfer of angular momentum from an excited to an unexcited molecule. The effect of this contribution has been shown to be of the order of about 1% or less at high energies [25c] and serves merely to smear out interferences between identical molecules. Unfortunately because of the violation of unitarity the distorted wave approximation is not reliable for calculating total integral cross sections.

Evidence for the complete neglect of the potential anisotropy comes from nearly exact close coupling calculations for He–H_2. Secrest and Eastes [26] and Fremerey and Toennies [27] have noted that the integral total cross section calculated for He–H_2 with an anisotropic potential at energies of the order of 1 eV is nearly identical to the elastic cross section calculated for the spherically symmetric angle averaged potential. McGuire [28] has investigated the effect of the anisotropic part of the potential on the integral cross section and comes to the conclusion that the anisotropic potential can be neglected if it has a shorter range than the spherical symmetric potential. This result indicates the conditions under which the law of conservation of cross section proposed by Levine [29] can be applied.

Thus the contribution from inelastic processes can be safely neglected[1] at beam energies less than the threshold for the least energetic rotational transition. The transitions and corresponding threshold beam velocities in the center of mass frame are p-H_2, $(j=0 \rightarrow j=2)$, $g=2940$ m/sec; D_2, $(j=0 \rightarrow j=2)$ $g=1470$ m/sec; HD, $(j=0 \rightarrow j=1)$ $g=1200$ m/sec. At higher velocities the situation is less clear but on the basis of the above discussion it seems reasonable to assume that inelastic processes contribute less than 1% to the cross sections at $v \leqq 2500$ m/sec.

In order to be able to use all of the available scattering data for the various isotopes we must examine possible isotope effects on the integral cross section. The intermolecular potentials of all combinations of H_2, HD, and D_2 are expected to show an isotopic effect in the van der Waals long range potential due to differences of the molecular polarizabilities [31]. Although the polarizabilities are independent of the nuclei the expectation value of the polarizability averaged over the vibrational motion is somewhat different because of the differences in vibrational wave function of the isotopic species. The resulting difference between the polarizability of H_2 and D_2 was measured by Hermans *et al.* [32] to be 1.26%. This is in good agreement with the value of 1.28% calculated for the $v=0, j=0$ state by Kolos and Wolniewicz [33]. The resulting difference in the dispersion forces is approximately 3%. The transport and the second virial coefficients of H_2 and D_2 have been interpreted to show this effect [34, 35]. In their extended discussion of the H_2-transport data Hanley *et al.* indicate, however, that the different transport data are not yet sufficiently consistent to deduce potentials of this accuracy and that, furthermore the simple two parameter potentials are not sufficiently flexible to fit the data over a large enough energy range. Thus we feel that this difference is not yet definitely established from the viewpoint of bulk property data.

At any rate the accuracy of our measurements does not make it possible to distinguish between the two cross sections, which we estimate to differ by only 1.2%[2]. We have therefore used all the available integral cross section data for H_2–H_2, D_2–H_2, D_2–D_2, and HD–D_2 to establish one and the same potential. The measured velocity dependence of the integral cross section of HD–HD [18b] deviates from the other isotopic systems, which can be explained by the lower symmetry of the HD molecule [36], and for this reason this data was not used.

The procedure used to determine the best fit potential is similar to that described elsewhere [21, 22a]. Elastic cross sections are first calculated for a

---

[1] Van de Ree [30] has recently observed a small cross section contribution from closed channels for He–D_2. The velocity averaged contribution is, however, less than about 1%.

[2] Using the Massey and Mohr approximation for a $V(R) = -\frac{C}{R^6}$ potential we have $\sigma \propto \left(\frac{C}{\hbar g}\right)^{2/5}$, where according to the London formula the dispersion constant C is proportional to the product of the polarizabilities $\alpha_1 \cdot \alpha_2$. For D_2–D_2 with a $\Delta C/C$ of 0.03 we get therefore $\Delta\sigma/\sigma \simeq 0.012$.

Table 2. χ^2 values for the comparison of 5 different beam experiments with 11 different literature potential models and our potential model

Authors	Ref.	ε [meV]	R_0 [Å]	R_m [Å]	C_6 [a.u.]	C_8 [a.u.]	χ_1^2	χ_2^2	χ_3^2	χ_4^2	χ_5^2	$\chi_{\mathrm{tot},k}^2$
Mason and Rice	[37]	3.21	2.97	3.34	13.0	0	27.6	18.1	24.3	41.3	14.4	125.7
Michels *et al.*	[38]	3.26	2.96	3.32	14.6	0	9.2	21.7	142.0	620.3	28.4	821.6
Diller and Mason[a]	[34]	3.31	2.97	3.33	15.2	0	3.6	21.7	21.9	36.6	14.0	97.8
[b]	[34]	3.11	2.98	3.34	14.5	0	14.3	33.6	48.6	77.1	18.8	192.4
Fisher	[39]	3.42	3.01	3.42	—	—	6.4	22.1	9.4	57.6	11.4	106.9
Gordon and Cashion	[43]	2.84	3.01	3.45	16.8	0	31.2	87.8	71.9	1367.7	17.7	1576.3
Hanley *et al.*[c]	[15]	3.38	2.97	3.33	15.4	0	5.0	22.5	15.3	31.0	13.1	86.9
[d]	[15]	2.62	3.06	3.50	12.2	0	12.8	42.5	75.0	149.0	28.0	307.3
Butz *et al.*	[18b]	3.12	2.94	3.30	13.5	0	46.4	38.6	31.6	92.6	20.5	229.7
Dondi *et al.*	[18a]	2.93	3.06	3.45	12.6[e]	0	29.0	141.7	75.4	212.0	21.2	479.3
Farrar and Lee	[17]	3.00	3.12	3.49	12.1	116.0	30.2	208.0	67.5	268.0	17.5	591.3
MSV potential, this work		3.10	3.045	3.42	11.8	110.0	3.0	16.0	15.0	31.0	12.0	77.0

Experiment 1: H_2–H_2 absolute cross sections, this work.
Experiment 2: HD–D_2 relative cross sections, Ref. [18b].
Experiment 3: D_2–H_2 relative cross sections, this work.
Experiment 4: D_2–D_2 relative cross sections, Ref. [18b].
Experiment 5: D_2–D_2 relative cross sections, this work.

[a] H_2–H_2 potential.
[b] D_2–D_2 potential.
[c] For low temperature data.
[d] For high temperature data.
[e] Estimated from the value of the potential at $R = 5.9$ Å.

potential model[3]. The cross sections are then corrected for the insufficient angular resolving power of the specific apparatus. This correction can be accurately calculated by weighting the theoretical differential cross section for the same potential with the effective probability that a particle which has been deflected by a laboratory angle Θ still strikes the detector. The corrected cross section is then averaged over the distribution of relative velocities. These corrected theoretical cross sections for an experimental setup j and for a potential $V_k(R)$ are denoted by $\bar{\sigma}_k^j$. They are then compared with the experimental cross section $\bar{\sigma}^j$ by calculating χ^2. The χ^2 for the j^{th} setup consisting of N_j measured cross sections compared with the potential $V_k(R)$ is defined by

$$\chi_k^{2,j} = \sum_{i=1}^{N_j} \left(\frac{\bar{\sigma}_k^j(v_i) - p_{jk}\bar{\sigma}^j(v_i)}{p_{jk}\Delta\bar{\sigma}^j(v_i)} \right)^2, \quad j = 1 \ldots M$$

where p_{jk} is a scaling factor which takes account of the unknown target density of the relative measurements and is chosen to minimize χ_k^2. For the absolute measurements p_{jk} was varied within the boundaries given by the systematic error of the target particle density. $\Delta\bar{\sigma}^j(v_i)$ is the statistical error of the single value. The M sets of experimental cross sections are combined to give

$$\chi^2_{\mathrm{tot},k} = \sum_{j=1}^{M} \frac{1}{q_j^2} \chi_k^{2,j}$$

with an error normalizing factor q_j^2 which is close to one and which is chosen to make this combination meaningful (see Ref. [21], p. 99). Table 2 lists the χ^2-values and some characteristic quantities of the potentials.

Table 2 shows that the integral cross section measurements agree better with the bulk property potentials (smaller χ^2 values) than with the two potentials obtained from differential cross section measurements. The better agreement with bulk property potentials is also shown in Fig. 3. There calculated integral cross sections for three different literature potential models are directly compared with our measurements. Despite the apparent good agreement of the bulk property potentials with our measurements these potentials have the drawback that the C_8 term was neglected. Thus the C_6 values are probably too large as is indicated by the lack of agreement with the semiempirical value of $C_6 = 12.08$ a.u. calculated by Starkschall and Gordon [13a]. For this reason we have made a new fit of the integral cross section data. Our potential model is a flexible multi parameter MSV potential model similar to that used by Farrar and Lee, and is given by

$$V(R) = \begin{cases} 4\varepsilon\{\exp(2\gamma(1 - R/R_0)) - \exp(\gamma(1 - R/R_0))\} & R < 3.5\,\text{Å} \\ \sum_{l=0}^{3} a_{kl}(R - R_k)^l & R_k \leqq R < R_{k+1} \\ -C_6 \cdot R^{-6} - C_8 \cdot R^{-8} & 5.4\,\text{Å} \leqq R\,. \end{cases}$$

In order to obtain a potential roughly consistent with the bulk property data we have kept the well volume, defined by $\int_{R_0}^{\infty} V(R)\,dR$, constant and approximately

---

[3] For the scattering of identical particles weighting factors for even and odd angular momentum were taken into account. See for example [18a].

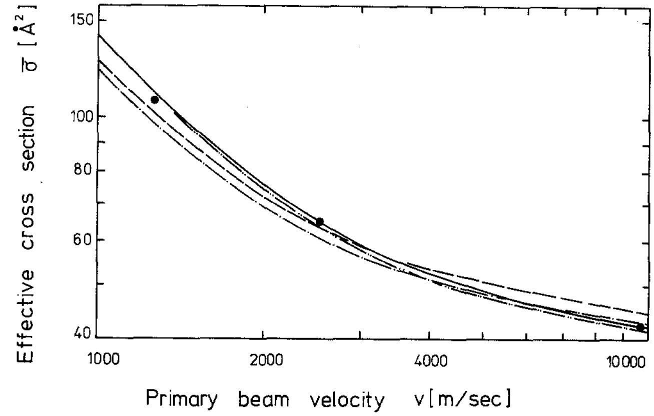

Fig. 3. The full circles show the three absolute effective total cross sections of H_2–H_2 at a target temperature of 77.3 °K. The solid curve shows the effective cross section computed with the MSV potential. The effective cross sections based on the potentials of Dondi *et al.* (–·–·–) and Farrar and Lee (– – – –), which are derived from differential cross section measurements, are not consistent with our relative and absolute results. The potential of Hanley *et al.* derived from transport coefficients at low temperature yields, however, an effective total cross section (–··–··–) which is in closer agreement to our result

equal to that of the bulk property potentials. This procedure seems justified since this quantity is measured absolutely in virial coefficient experiments. Furthermore we have set the long range dispersion constants C_6 and C_8 equal to the values calculated by Starkschall and Gordon ($C_6 = 12.08$ a.u.) [13a] and Margenau ($C_8 = 113.5$ a.u.) [1b], respectively. In the course of the fitting procedures it was observed that χ^2 could be reduced somewhat by varying C_6 and C_8 slightly within the error limits given in the theoretical calculations. As indicated by the χ^2 values (Table 2) our MSV potential is comparable to that of Diller and Mason[a] and Hanley *et al.*[c] but has the advantage over these potentials that the long range part is in better agreement with theory.

The parameters

$$\varepsilon = 3.10 \text{ meV}$$

$$R_0 = 3.045 \text{ Å}$$

$$\gamma = 5.55$$

and the spline coefficients a_{kl} (in meV Å^{-l})

l / k	0	1	2	3	R_k
1	−3.050	1.122	2.558	−2.078	3.5
2	−2.109	2.122	−0.558	−0.0274	4.0

provide the best fit with $C_6 = 11.8$ a.u. and $C_8 = 110$ a.u. This potential is a later version of our potential cited by Farrar and Lee [17]. It is displaced a little to smaller distances. The fit of the relative values is shown in Fig. 2 and of the absolute values in Fig. 3. The χ^2 values for our potential are also listed in the last row of

Table 2. As can be concluded from local potential variations the relative values are especially sensitive to the potential well and the lower part of the repulsive potential. The absolute value at $v = 9630$ m/sec determines the potential in the region of 150 meV. For a more detailed discussion of the potential regions probed in integral cross section measurements see [40].

Discussion

A graphical comparison between our MSV-potential and potentials from bulk properties shown in Figs. 4 and 5 demonstrate a partial agreement in the repulsive region. The potential wells are, however, quite differently shaped. Our potential is flatter and broader than the commonly used model potentials. Figures 6 and 7 show that our MSV potential and the potential of Dondi *et al.* also differ significantly in the well region, whereas the repulsive potential is nearly identical. The large χ^2 of the potential of Dondi *et al.* is due only to the differences in the well region thus possibly indicating the greater sensivity of the integral cross section data to the potential well. The potential of Farrar and Lee is different from the MSV potential in the entire potential region. The smaller potential well and the stronger repulsion causes a smaller fall off with velocity of the integral cross section. At $v = 1270$ m/sec the cross section computed with this potential is 7% smaller than our experimental values, whereas it is 4% larger at $v = 9650$ m/sec. However, the differential cross sections computed with the earlier version of our potential and Farrar and Lee's potential do not differ significantly (Fig. 5, Ref. [17]).

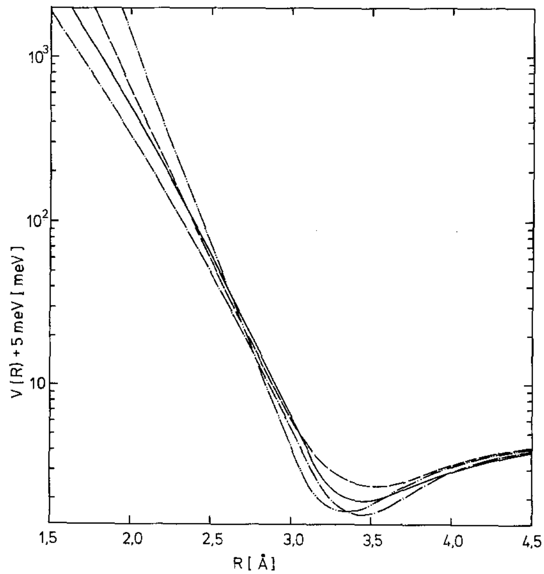

Fig. 4. A comparison between our MSV potential (———) and potentials from bulk properties [(– –) high temperature and (–··–··–) low temperature of Hanley *et al.*; (–·–·–) Fisher] illustrates that our potential is not quite different in magnitude from the gaseous properties result

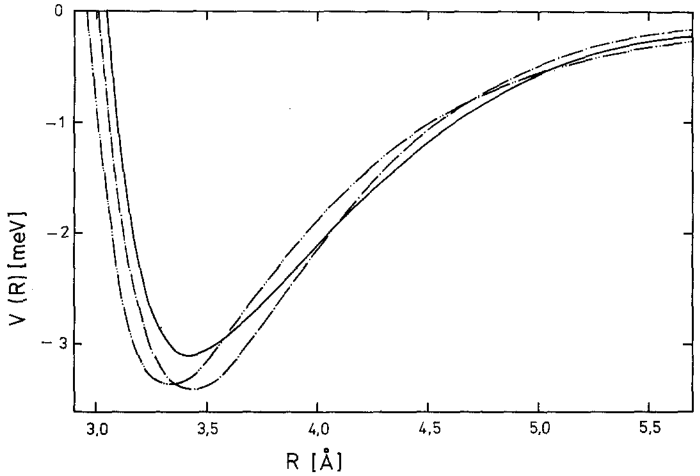

Fig. 5. Potential wells of the potentials from Fig. 4. During the fitting procedure we have tried to keep the well volume constant and equal to the bulk property result

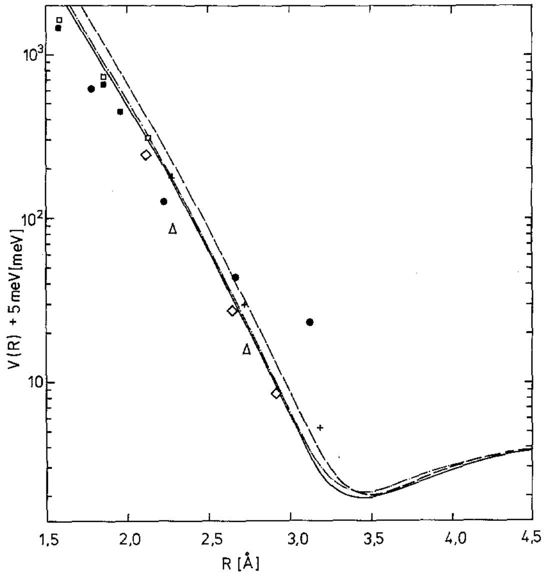

Fig. 6. Comparison between the repulsive potentials from scattering experiments [Farrar and Lee (–––), Dondi *et al.* (—·—), our work (————)] and theoretical potential values for fixed nuclei, averaged over three or four geometrical orientations of the molecules (△ Evett and Margenau, + Mason and Hirschfelder, □ Patch, ● Abrams, ◇ Kochanski, ■ Silver and Stevens)

In the well region our results are closest to the theoretical values of Evett and Margenau and Kochanski averaged to give a spherical symmetric potential. As shown in Fig. 7 the latest *ab initio* values of Meyer are approximately 10% smaller in the well region. Since the CEPA-method, used by Meyer, does not overestimate the correlation energy as is the case in the IEPA method, our somewhat larger

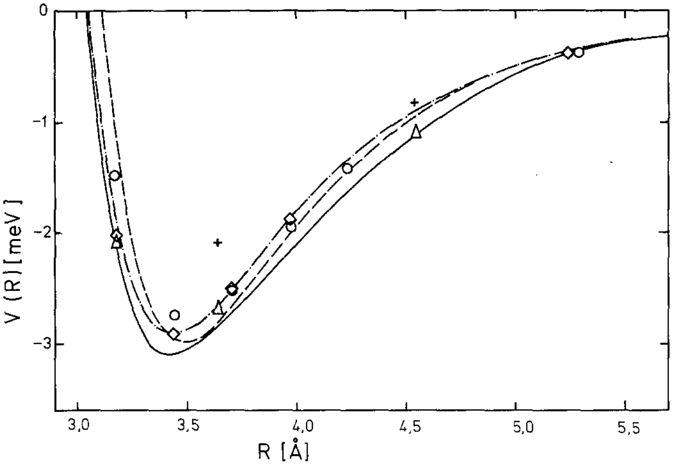

Fig. 7. Comparison between the potential wells from scattering experiments [Farrar and Lee (– – –), Dondi *et al.* (–·–·–) and our work (———)] and from calculations [△ Evett and Margenau, + Mason and Hirschfelder, ◇ Kochanski, ○ Meyer). Dondi's potential differs significantly from our potential in the well region, whereas in the repulsive part the two potentials are nearly identical (Fig. 6). The great difference of the χ^2 values for these two potentials illustrates the sentivity of the measured cross sections to the well region

value for ε seems consistent with these calculations[4]. The averaged theoretical values at fixed nuclei for the repulsive potential are compared with our results in Fig. 6. The good agreement with the valence bond values of Patch and the CI-results of Silver and Stevens is remarkable. The perturbation values of Kochanski are also very close to our results.

In the scattering calculations the phase shift for both the *s*-wave ($l=0$) and the *p*-wave ($l=1$) are observed to approach π with decreasing scattering energies. Thus our MSV potential has a bound state for H_2–H_2 in both the $l=0$ and $l=1$ states. Since a large part of the well region is described by a Morse potential model the energy of the bound state can be estimated from the Morse formula [41]:

$$E_n = -\left[\frac{(2\mu\varepsilon)^{\frac{1}{2}} R_0}{\gamma\hbar} - (n+1/2)\right]^2 \frac{\gamma^2\hbar^2}{2R_0^2\mu}.$$

The result for the bound state energy is $E_1 = -1.58\,\mathrm{cm}^{-1}$. The MSV potential, which is slightly deeper in the long range van der Waals tail than the pure Morse potential, is expected to yield a stronger bound state. Measurements of the infrared absorption spectrum of H_2–H_2 by Watanabe and Welsh [42] are consistent with a bound state at a level of 2–3 cm^{-1} [43] in reasonable agreement with our result.

Finally in Fig. 8 we compare the spherical symmetric potentials of the four electron closed shell systems He–He, He–H_2, and H_2–H_2. The potential for He–He is from the integral cross section measurements of Bennewitz *et al.* [24] and the potential for He–H_2 from our own earlier work [20a]. The potentials are

---

[4] This is in agreement with the observation that the calculated ε for He–H_2 using the IEPA method [20b] and for He–He [22a] are larger than the measured values (H_2–He) (He–He) [20a, 22a, 24].

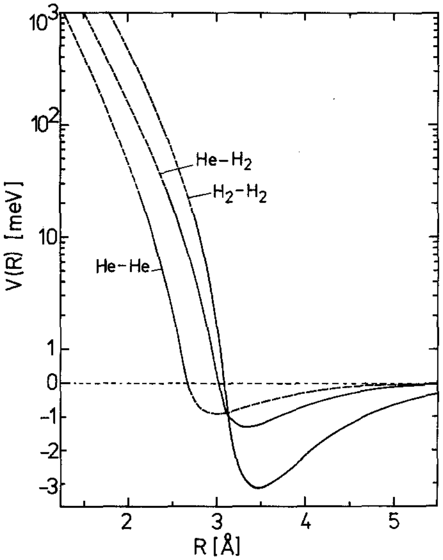

Fig. 8. Comparison of the experimentally measured potentials for the four electron systems. For values $V > 1$ meV the curves are drawn with a logarithmic scale, and for values $V < 1$ meV with a linear scale. The solid part of each curve shows the region probed in these experiments

similar in shape. The differences in magnitude can be explained by the greater size and polarizability of the H_2 molecule compared to the He-atom. The former leads to an increase in R_0 and the latter to a greater dispersion interaction and a greater well depth. Table 3 summarizes the potential parameters of these three systems. Also shown is a comparison of the measured parameters for He–H_2 with those estimated from the simple combining rules: $\varepsilon_{12} = \sqrt{\varepsilon_1 \cdot \varepsilon_2}$ and $R_{m_{12}} = (R_{m_1} + R_{m_2})/2$. The limited success of the combining rules in predicting ε is not surprising in view of the large differences in ε for the symmetric interactions.

Summary

The velocity dependence and the absolute magnitude of the total integral cross section for n-H_2–n-H_2 has been measured. All of the available integral cross section data was fitted to a multiparameter spherically symmetric potential, which is consistent with bulk property measurements. There is a small, but probably

Table 3. Potential parameters for the four-electron closed shell systems for the MSV-potential

System	Ref.	ε [meV]	R_0 [Å]	R_m [Å]	γ
He–He	[24]	0.888	2.685	2.979	5.43
He–H_2	[20a]	1.34	3.001	3.37	5.40
H_2–H_2	this work	3.10	3.045	3.42	5.55
He–H_2	simple combining rules	1.65	—	3.20	—
He–H_2	combining rule of [44]	1.592	—	3.20	—

significant, difference between this potential and that from differential cross section measurements for n-H_2–n-H_2 and para-H_2–para-H_2. Measurements of integral cross sections for para-H_2–para-H_2 are in progress and may serve to clear up the small difference.

Acknowledgements. This research was made possible by the generous support of the Deutsche Forschungsgemeinschaft. We also wish to thank H. G. Bennewitz, H. Busse, H. D. Dohmann, W. auf'm Kampe, and D. E. Oates of the Bonn molecular beam group for lending us their apparatus for the experiments at low target temperatures and for their help with these measurements. We also wish to thank W. Meyer (Stuttgart, now Mainz) for sending us his theoretical results prior to publication. Finally we thank W. Bauer, B. Lantzsch, and K. Walaschewski for commenting on the manuscript.

Note Added in Proof. Two recent papers on H_2–H_2 are of interest: Monchick [Chem. Phys. Letters **24**, 91 (1974)] has proposed a new potential from bulk data with an $R_0 = 2.96$ Å, $R_m = 3.33$ Å and $\varepsilon = 3.26$ meV. Zarur and Rabitz [J. Chem. Phys. **60**, 2057 (1974)] report an approximate close coupling calculations of elastic and inelastic differential and integral cross sections for para-para, ortho-para and ortho-ortho collisions.

References

1a. de Boer, J.: Physica **9**, 363 (1942)
1b. Evett, A. A., Margenau, H.: Phys. Rev. **90**, 1021 (1953)
Evett, A. A., Margenau, H.: J. Chem. Phys. **21**, 958 (1953)
Margenau, H.: Phys. Rev. **63**, 385 (1943)
1c. Mason, E. A., Hirschfelder, J. O.: J. Chem. Phys. **26**, 756 (1957)
2. Kochanski, E.: J. Chem. Phys. **58**, 5823 (1973)
3. Mascagno, V., Musso, G. F.: J. Chem. Phys. **46**, 4015 (1967)
Mascagno, V., Musso, G. F.: J. Chem. Phys. **47**, 1723 (1967)
Mascagno, V., Musso, G. F.: J. Chem. Phys. **48**, 2657, 2834 (1968)
Mascagno, V., Musso, G. F.: J. Chem. Phys. **50**, 571 (1969)
Mascagno, V., Musso, G. F., McWeeny, R.: J. Chem. Phys. **47**, 4617 (1967)
4. Patch, R. W.: J. Quantum Spectry. Radiat. Transfer **11**, 1331 (1971)
5. Vanderslice, J. T., Mason, E. A.: J. Chem. Phys. **33**, 492 (1960)
6. Abrams, R. B., Patel, J. C., Ellison, F. O.: J. Chem. Phys. **49**, 450 (1968)
7. Tapia, O.: Chem. Phys. Letters **10**, 613 (1971)
Tapia, O., Bessis, B., Bratoz, S.: Int. J. Quantum Chem. **4**, 289 (1971)
8. Wilson, C. W., Goddard, W. A.: J. Chem. Phys. **51**, 716 (1969)
Wilson, C. W., Goddard, W. A.: J. Chem. Phys. **56**, 5913 (1972)
9. Rubinstein, M., Shavitt, I.: J. Chem. Phys. **51**, 2014 (1969)
10. Bender, C. F., Schaefer, H. F.: J. Chem. Phys. **57**, 217 (1972)
11. Meyer, W.: Private communication
12. Silver, D. M., Stevens, R. M.: J. Chem. Phys. **59**, 3378 (1973)
13a. Starkschall, G., Gordon, R. G.: J. Chem. Phys. **54**, 663 (1971)
13b. Victor, G. A., Dalgarno, A.: J. Chem. Phys. **50**, 2535 (1969)
13c. Victor, G. A., Dalgarno, A.: J. Chem. Phys. **53**, 1316 (1970)
14a. Langhoff, P. W., Gordon, R. G., Karplus, M.: J. Chem. Phys. **55**, 2126 (1971)
14b. Kochanski, E.: Chem. Phys. Letters **10**, 543 (1971); **15**, 254 (1972)
15. Hanley, H. J. M., McCarty, R. D., Intemann, H.: J. Res. Natl. Bur. Std. **74A**, 331 (1970)
16. Leonas, V. B., Sermyagin, A. V., Kamyshov, N. V.: Chem. Phys. Letters **8**, 282 (1971)
17. Farrar, J. M., Lee, Y. T.: J. Chem. Phys. **57**, 5492 (1972)
18a. Dondi, M. G., Valbusa, U., Scoles, G.: Chem. Phys. Letters **17**, 137 (1972)
18b. Butz, H. P., Feltgen, R., Pauly, H., Vehmeyer, H.: Z. Physik **247**, 70 (1971)
19. Toennies, J. P.: In: Eyring, H., Henderson, D., Jost, W. (Eds.): Physical chemistry, an advanced treatise, Vol. IV. New York: Academic Press 1974
20a. Gengenbach, R., Hahn, Ch.: Chem. Phys. Letters **15**, 604 (1972)
20b. Tsapline, B., Kutzelnigg, W.: Chem. Phys. Letters **23**, 173 (1973)

21. Gengenbach, R., Hahn, Ch., Toennies, J. P.: Phys. Rev. A 7, 98 (1973)
22a. Gengenbach, R., Hahn, Ch., Welz, W.: To be published
22b. Bennewitz, H. G., Dohmann, H. D.: Vakuum Tech. **14**, 8 (1965)
22c. Bennewitz, H. G., Schrader, W.: To be published
23. Feltgen, R., Pauly, H., Torello, F., Vehmeyer, H.: Phys. Rev. Letters **30**, 820 (1973)
24. Bennewitz, H. G., Busse, H., Dohmann, H. D., Oates, D. E., Schrader, W.: Z. Physik **253**, 435 (1972)
25a. Davison, W. D.: Discussions Faraday Soc. **33**, 71 (1962)
25b. Davison, W. D.: Proc. Roy. Soc. (London) A **280**, 227 (1964)
25c. Bauer, W.: Max-Planck-Institut für Strömungsforschung, Ber.-Nr. 145 (1973)
26. Eastes, W., Secrest, D.: J. Chem. Phys. **56**, 640 (1972)
27. Fremerey, H., Toennies, J. P.: To be published
28. McGuire, P.: To be published
29. Levine, R. D.: Chem. Phys. Letters **4**, 309 (1969); J. Chem. Phys. **57**, 1015 (1972)
30. van de Ree, J.: Private communication
31. Knaap, H. F. P., Beenakker, J. J. M.: Physica **27**, 523 (1961)
32. Hermans, L. J. F., De Groot, J. J., Knaap, H. F. P., Beenakker, J. J. M.: Physica **31**, 1567 (1965)
33. Kolos, W., Wolniewicz, L.: J. Chem. Phys. **46**, 1426 (1967)
34. Diller, D. E., Mason, E. A.: J. Chem. Phys. **44**, 2604 (1966)
35. Mason, E. A., Amdur, I., Oppenheim, I.: J. Chem. Phys. **43**, 4458 (1965)
36. van Montfort, J. Th., Heukels, W. F., van de Ree, J.: J. Chem. Phys. **57**, 947 (1972)
37. Mason, E. A., Rice, W. E.: J. Chem. Phys. **22**, 522 (1954)
38. Michels, A., de Graaf, W., ten Seldam, C. A.: Physica **26**, 393 (1960)
39. Fisher, B. B.: Calculations of the thermal properties of hydrogen, LA-3364. Los Alamos Scientific Laboratory, Los Alamos, New Mexico, USA (1965)
40. Bickes, Jr., R. W., Lantzsch, B., Toennies, J. P., Walaschewski, K.: Discussions Faraday Soc. **55**, 167 (1973)
41. Morse, P. M.: Phys. Rev. **34**, 57 (1929)
42. Watanabe, A., Welsh, H. L.: Phys. Rev. Letters **13**, 810 (1964)
43. Gordon, R. G., Cashion, J. K.: J. Chem. Phys. **44**, 1190 (1966)
44. Hudson, H. G., McCoubrey, J. C.: Trans. Faraday Soc. **56**, 761 (1960)

Prof. Dr. J. P. Toennies
Max-Planck-Institut für Strömungsforschung
D-3400 Göttingen
Böttingerstr. 6–8
Federal Republic of Germany